

Optics Letters

Optical center of a luminescent solar concentrator: supplement

JINGJIAN ZHOU,^{1,*}  JING HUANG,^{1,2,3} AND ILYA SYCHUGOV^{1,4} 

¹Department of Applied Physics, KTH - Royal Institute of Technology, Stockholm 11419, Sweden

²School of Environmental and Biological Engineering, Nanjing University of Science and Technology, Nanjing 210094, China

³e-mail: jinghuang@njust.edu.cn

⁴e-mail: ilyas@kth.se

*Corresponding author: jingjian@kth.se

This supplement published with Optica Publishing Group on 21 September 2022 by The Authors under the terms of the [Creative Commons Attribution 4.0 License](https://creativecommons.org/licenses/by/4.0/) in the format provided by the authors and unedited. Further distribution of this work must maintain attribution to the author(s) and the published article's title, journal citation, and DOI.

Supplement DOI: <https://doi.org/10.6084/m9.figshare.20737012>

Parent Article DOI: <https://doi.org/10.1364/OL.467917>

Supporting Information

Optical Center of a Luminescent Solar Concentrator

JINGJIAN ZHOU¹, JING HUANG^{1, 2, *}, ILYA SYCHUGOV^{1, *}

¹Department of Applied Physics, KTH - Royal Institute of Technology, Stockholm 11419, Sweden

²School of Environmental and Biological Engineering, Nanjing University of Science and Technology, Nanjing 210094, China

*Corresponding author: ilyas@kth.se; jinghuang@njust.edu.cn

Calculated average optical paths for an isotropic emitter

Optical path lengths from isotropic emitters at different distances from the geometrical center were calculated. Rays were emanating with half-a-degree step. Point positions were chosen both along the orthogonal axes and the diagonal of the square with $0.001 \times a$ step. The frequency count of the optical paths was performed and the average value of this distribution was taken for each position. The averaged value between the points on axes and on diagonal directions is presented.

Excitation position-dependent measurements

At each edge, 8 pieces of small-sized Si solar cells (KXOB25, Anysolar, $21 \times 6.6 \text{ mm}^2$ active area) are attached, connected in parallel. In each piece of solar cell, 4 p-n junctions are connected in series, capable of delivering $\sim 14 \text{ mA}$ short circuit current (I_{sc}) and $\sim 2.7 \text{ V}$ open circuit voltage (V_{oc}) under AM1.5G. Note that solar cells are firmly attached to the LSC edges by using pure OSTE as glue and there are no air gaps in between. Our LED-based solar simulator (Sunbrick from G2V optics, ASTM E927 class AAA+, $25 \times 25 \text{ cm}^2$) simulates sunlight from 360 nm to 1120 nm with a spectral mismatch of less than 5%.

A set of frontside masks with open windows ($1 \times 1 \text{ cm}^2$, distributed from center to the edge, perpendicular to the edge), as shown in the inset of Fig. 2(a), were used to shift the position of point excitations. Only one window was kept open at a time and others were covered by black tapes. The frontside mask can spin on the device to access different directions. Besides, a backside light-absorbing mask was used to minimize the impact from back reflections. Ideally, the light should only enter from the open window. Note that both masks do not directly touch the device ($\sim 5 \text{ mm}$ in distance), thereby not interrupting the total internal reflection of waveguided light. To eliminate the impact from the possible non-uniformity of simulated sunlight, the open window was always put at the same position under the solar simulator by shifting the device. At the plane of standard AM1.5G, the mobility of this device is limited by the mechanical structure of solar simulator. Instead, 0.9 AM1.5G was applied for the following measurements, which is at $\sim 5\text{-}6 \text{ cm}$ lower plane. To exclude the effect of temperature, all the I_{sc} values were recorded immediately after the exposure to sunlight (it took at least half an hour for the solar simulator to stabilize before measurements).

Optical characterizations of the device

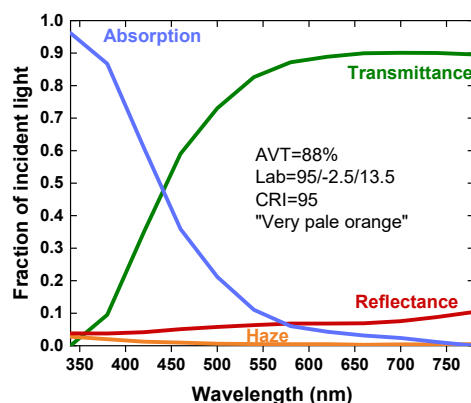


Fig. S1. Transmittance, absorption, reflection and haze spectra of the used LSC.

In the LSC, ~60 mg Si QDs are homogeneously dispersed in the polymer interlayer. According to the color coordinate, the device has a “very pale orange” tint (Colorhexa) [1]. With the emission peak wavelength at 870 nm, a large Stokes shift is present, translating to a negligible reabsorption loss. In addition, the extremely low haze implies a negligible scattering loss.

Estimated absorption fraction of the solar spectrum

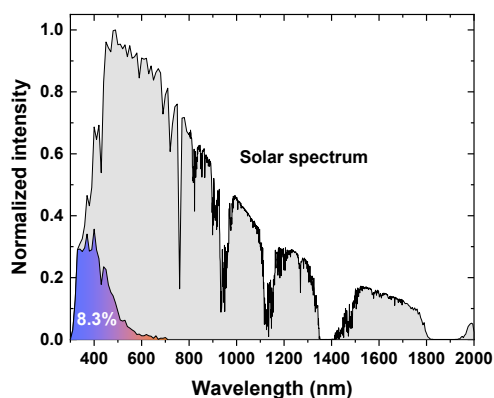


Fig. S2. Absorption fraction under solar spectrum.

According to the measured absorption, this LSC absorbs a fraction of 8.3% sunlight power (absorption above 1000 nm not shown).

Effect of the size of solar cells

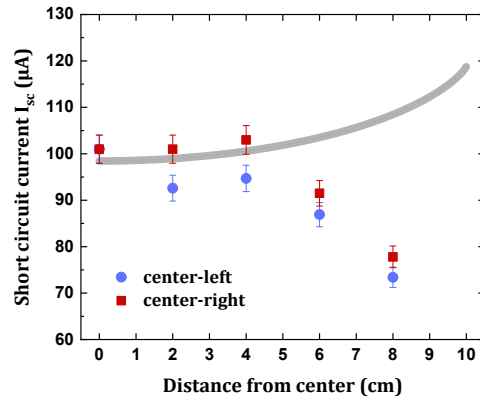


Fig. S3. Short circuit current under point excitations along two directions (center-left in blue and center-right in red) of another $20 \times 20 \text{ cm}^2$ LSC attached with longer solar cells. The grey solid line indicates the predicted trend (given an initial I_0 value).

For this LSC (2nd device), 8 pieces of solar cells are connected in parallel to cover its edges. Each solar cell consists of 8 pieces of p-n junctions connected in series. As can be seen, it shows a dropping trend of short circuit current when the illumination window gets close to the edge. This is attributed to the low detection resolution of the large size solar cells, as illustrated in Fig. S4. Due to the fact that in this solar cell 8 pieces of p-n junctions are connected in series, the short circuit current will be limited by the lowest I_{sc} among p-n junctions, which corresponds to the longest optical path from the excitation point (red lines in Fig S4, left). This limitation becomes dominant when the illumination window is close to the edge (left). While for a small size of solar cell (right), this effect has a low impact.

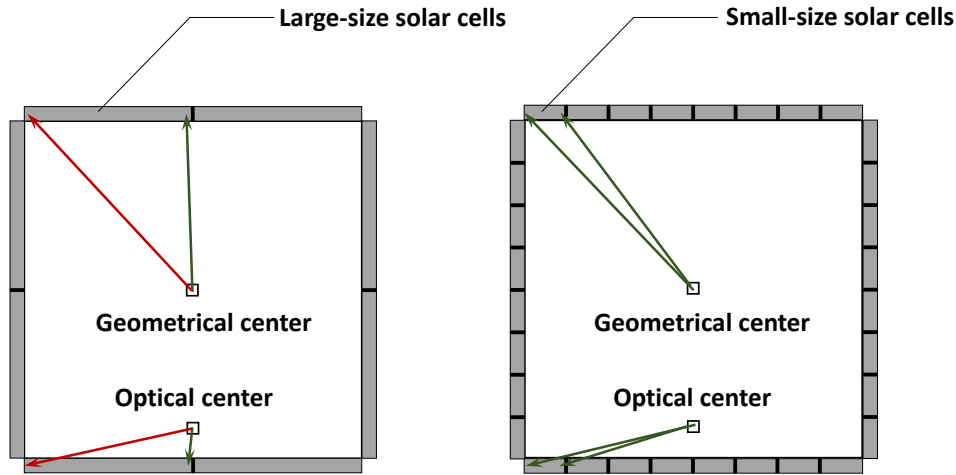


Fig. S4. Schematics of the resolution provided by different solar cell coupling at the edges: (left) 2nd device with long solar cells, and (right) the main device reported in this work with short solar cells connected in parallel. Irradiance within one solar cell is relatively uniform, which is nearly independent on the excitation spot position (green lines).

Estimation of the open circuit voltage and fill factor

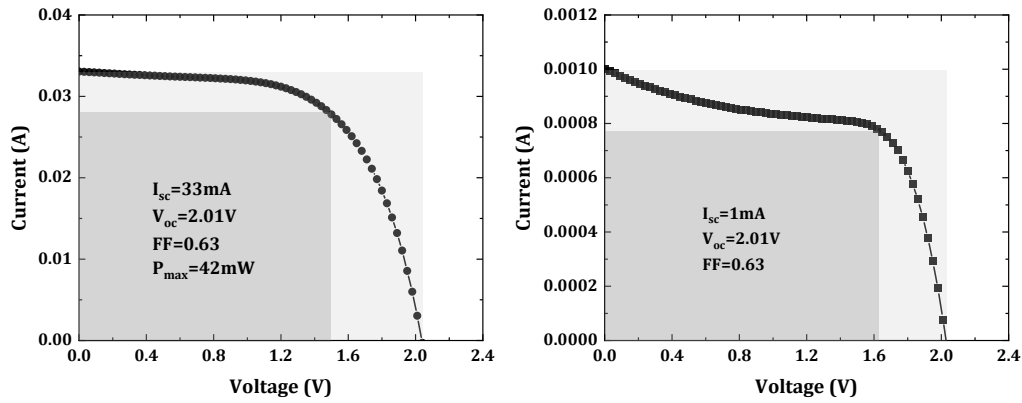


Fig. S5. I-V characteristic curves of the LSC under uniform illumination (left) and single solar cell delivering $\sim 1 \text{ mA}$ short circuit current (right).

By mimicking the irradiance on a single solar cell, almost the same open circuit voltage and fill factor can be obtained.

Another method estimating V_{oc} and FF

The relationship between the open circuit voltage (V_{oc}) of silicon solar cells and the incident irradiance (E) can be easily calibrated by a set of data measured under the solar simulator based on a well-known dependence $V_{oc} = V_0 - a \ln(E_0 / E)$ [2]. For the solar cells used here, $V_0 = 2.5 \text{ V}$, $E_0 = 1000 \text{ W/m}^2$, $a = 0.203$. Then, extracting irradiance level from the measured LSC solar cell short circuit current, one can predict the open circuit voltage. As a reference, the I_{sc} of single piece of solar cell under one sun (1000 W/m^2 in irradiance) was measured to be 13 mA . With 32 mA total I_{sc} of the LSC-attached solar cells one can estimate on average that each piece of solar cells here contributes to $\sim 1 \text{ mA}$ (32 pieces in parallel). Since the short circuit current increase with the incident irradiance linearly, the irradiance on a single LSC-attached solar cell can be estimated as 77 W/m^2 . Thus, the estimated V_{oc} from equation above is $\sim 1.98 \text{ V}$ ($\sim 2\%$ error to the measured one 2.01 V). Finally, from the specifications of solar cells, an average fill factor (~ 0.65) can be used for the estimation of PCE.

Reference

1. C. Yang, D. Liu, and R. R. Lunt, *Joule* **3**, 2871-2876 (2019).
2. V. Lo Brano, A. Orioli, G. Ciulla, and A. Di Gangi, *Sol. Energy Mater. Sol. Cells* **94**, 1358-1370 (2010).